

Photon-assisted tunneling through a quantum dot

L. P. Kouwenhoven, S. Jauhar, K. McCormick, D. Dixon, and P. L. McEuen
*Department of Physics, University of California at Berkeley, Berkeley, and Materials Science Division,
 Lawrence Berkeley Laboratories, Mail Stop 2-200, Berkeley, California 94720*

Yu. V. Nazarov and N. C. van der Vaart
Department of Applied Physics, Delft University of Technology, 2600 GA Delft, The Netherlands

C. T. Foxon*
Philips Research Laboratories, Redhill, Surrey RH1 5HA, United Kingdom
 (Received 15 March 1994)

We study single-electron tunneling in a two-junction device in the presence of microwave radiation. We introduce a model for numerical simulations that extends the Tien-Gordon theory for photon-assisted tunneling to encompass correlated single-electron tunneling. We predict sharp current jumps which reflect the discrete photon energy hf , and a zero-bias current whose sign changes when an electron is added to the central island of the device. Measurements on split-gate quantum dots show microwave-induced features that are in good agreement with the model.

An oscillating potential with frequency f changes the energy E of an electron state into a set of energies $E + nhf$ with $n=0, \pm 1, \pm 2, \dots$. These so-called sideband energies can lead to electron tunneling that involves the emission ($n < 0$) and absorption ($n > 0$) of photons. The formation of sidebands has been important for many time-dependent transport studies addressing issues such as photon-assisted tunneling of quasiparticles in superconducting junctions,¹ the tunneling time,² and time-dependent resonant tunneling.³ Recent theoretical work has begun to focus on the effects of an oscillating potential on transport through small capacitance devices where the charging energy regulates the tunnel processes.⁴⁻⁷ For instance, Bruder and Schoeller⁷ have calculated the photoresponse of a two-level system. However, little theoretical work exists on realistic systems, e.g., quantum dots with many quantum levels,⁸ and no experiments have been reported except at very low frequencies.⁹

In this paper, we present numerical simulations and experiments on photon-assisted tunneling through a quantum dot. We assume a continuous single-particle density of states, i.e., a metallic system with an equivalent single electron circuit shown in the inset of Fig. 1. Our model extends the Tien-Gordon theory¹ to include the correlated tunneling of single electrons through a two-junction device. This model predicts discrete photon features, and is in agreement with measurements on split-gate quantum dot devices irradiated by 19-GHz microwaves.

We model the microwaves as an oscillating potential $\bar{V} \cos(2\pi ft)$ of the central island relative to the source and drain leads. To allow for an asymmetry in the ac coupling, we model the microwave amplitude by two parameters $\alpha_i = e\bar{V}_i/hf$, $i=s,d$ where \bar{V}_s and \bar{V}_d are the ac voltage drops across the source and drain junctions. Analogous to the Tien-Gordon description, we write the tunnel rate $\bar{\Gamma}_i$ in the presence of microwaves in terms of the rate Γ_i without microwaves as

$$\bar{\Gamma}_i(\varepsilon_i) = \sum_{n=-\infty}^{+\infty} J_n^2(\alpha_i) \Gamma_i(\varepsilon_i + nhf), \quad (1)$$

where the J_n 's are Bessel functions of the first kind. The rate without microwaves is given by the standard expression for small capacitance junctions $\Gamma_i(\varepsilon) = (G_i/e^2)\varepsilon_i / \{1 - \exp(-\varepsilon_i/k_B T)\}$.¹⁰ G_i is the conductance of the junction. ε_i is the energy difference between initial and final states, and is usually expressed as a function of capacitances and applied voltages.¹⁰ Equation (1) is valid for $\bar{\Gamma}_i \ll f$, such that the sideband energies have stationary occupation probabilities given by the Bessel functions. We also assume energy relaxation between tunnel events, which again allows the en-

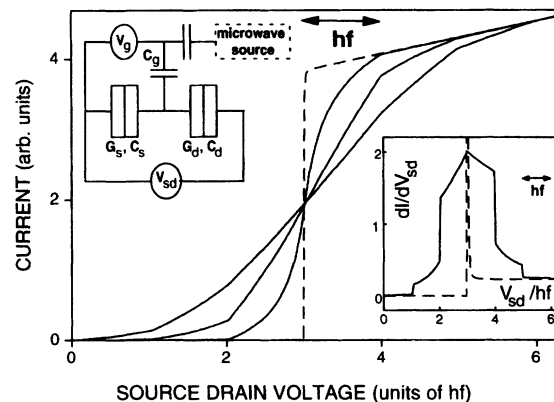


FIG. 1. Calculated $I-V_{sd}$ for the double-junction circuit shown in the upper-left inset for $G_s = 1000G_d$ and $C_s = C_d = 0.3C_g$ at zero temperature. The dashed curve is the Coulomb step without microwaves. The solid curves correspond to ac amplitudes $\alpha_s = \alpha_d = 0.7, 1.7, 2.7$. The arrow indicates the photon energy hf . The lower-right inset shows the differential conductance dI/dV_{sd} for amplitudes $\alpha_s = \alpha_d = 0$ (dashed) and 1.7 (solid).

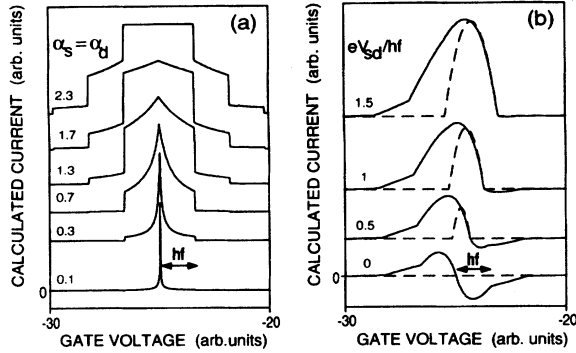


FIG. 2. Calculated $I-V_g$ for $G_s = G_d$ and $C_s = C_d = 0.3C_g$ at zero temperature. The conversion of the gate voltage scale to energy in units of hf is indicated by the arrow. Different curves have been offset for clarity. (a) $eV_{sd}/hf = 0.001$ and different curves correspond to ac amplitudes $\alpha_s = \alpha_d = 0.1, 0.3, 0.7, 1.3, 1.7, 2.3$. (b) Asymmetric ac coupling $\alpha_d = 0$ and $\alpha_s = 1.7$. The different curves correspond to $eV_{sd}/hf = 0, 0.5, 1, 1.5$.

ergies ε_i to be used in calculating the current. The net current is determined by the difference in the forward and backward rates through the source or through the drain junction, which we calculate by incorporating Eq. (1) into a standard computer model for Coulomb blockade that keeps track of all possible tunnel events.

Figure 1 shows a calculation of current versus source-drain voltage ($I-V_{sd}$) characteristics. The dashed curve is without microwaves and shows the first step of the Coulomb staircase. The solid curves show the effects of photon-assisted tunneling with increasing microwave amplitude ($\alpha_s = \alpha_d$). The current does not feature sharp jumps as in the case of a superconducting junction¹ or the case of a two-level system.⁷ Instead, at photon energies away from the nonlinearity, “kinks” are seen. Photon steps do become visible, however, in the differential conductance dI/dV_{sd} (see lower-right inset).

Discrete photon features are also found in calculated current versus gate voltage characteristics. Figure 2(a) shows a single Coulomb oscillation at small V_{sd} ($eV_{sd} \ll hf, e^2/C_{tot}$, $C_{tot} = C_s + C_d + C_g$) for different values of equal ac amplitudes $\alpha_s = \alpha_d$. Sharp jumps in the current occur at gate voltages which correspond to integer photon energies away from the central peak. The conversion of the gate voltage scale to energy in units of hf is indicated by the arrow. The slope of the current jumps is governed by eV_{sd} and $k_B T$, and thus to obtain sharp features these should be small compared to hf . From additional calculations we find that the sharp photon structure does not depend on the conductance ratio G_s/G_d .

In Fig. 2(b) we show results for completely asymmetric coupling, with $\alpha_s = 1.7$ and $\alpha_d = 0$. Here, we show the dependence on increasing V_{sd} . The dashed curves illustrate the peak broadening without microwaves due to increasing V_{sd} . The corresponding solid curves show the total current in the presence of microwaves. For $V_{sd} \neq 0$, asymmetric coupling of the microwaves leads to an asymmetric broadening of the Coulomb peaks. On one side of the peak photon-assisted tunneling leads to extra positive current and on the

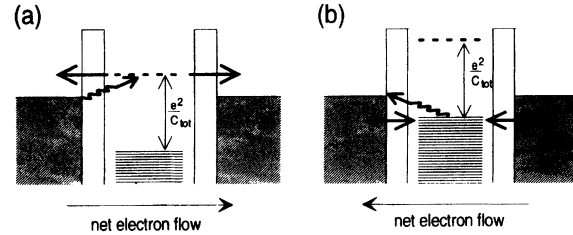


FIG. 3. Energy diagram for $V_{sd} = 0$ and photon-assisted tunneling through only the left barrier. In (a) the resulting electron flow is from left to right, while in (b) it is from right to left.

other side to extra negative current. Upon increasing V_{sd} the negative current gradually disappears. Although $V_{sd} = 0$ for the lowest curve, we still find a nonzero current. This means that if photon-assisted tunneling occurs through one barrier and normal tunneling through the other barrier, the dot operates as an electron pump (see also Ref. 7, and, for a double-barrier structure without Coulomb interaction, Ref. 11).

To understand the above numerical results, consider the two energy diagrams in Figs. 3(a) and 3(b). These diagrams correspond to being just to the right [3(a)] or left [3(b)] of a Coulomb peak where, in the absence of microwaves, no current flows due to the Coulomb blockade. Photon-assisted tunneling is required to induce a current. This process is represented by oscillating arrows from an initial energy state to a higher final state. For simplicity, we illustrate the case of zero source-drain voltage and completely asymmetric ac coupling ($\alpha_s \neq 0$, $\alpha_d = 0$). In Fig. 3(a), tunneling into the dot only occurs via photon absorption through the left barrier. Tunneling out of the dot can occur through both barriers. Tunneling out through the right barrier induces a nonzero net electron flow from left to right, which is the pumped current. By changing V_g the dashed level can be pulled below the Fermi energies of the reservoirs as shown in Fig. 3(b). Without microwaves this would correspond to moving through a Coulomb peak and thus adding an electron to the dot. Now, once inside, an electron can only tunnel out of the dot through the left barrier via photon absorption. Tunneling into the dot can occur through both barriers. The net electron flow is now from right to left. The asymmetric coupling in Fig. 3 thus causes the dot to operate as an *electron-photon pump*.

The numerical results of Fig. 2(b) show that asymmetric ac amplitudes do not lead to sharp current jumps in the $I-V_g$ characteristics. In contrast, for the symmetric ac amplitude case of Fig. 2(a) the only asymmetry comes from the energy difference V_{sd} between the two reservoirs. Only electrons from this small energy interval ($eV_{sd} \ll hf$) give rise to a net current flow. There is a sharp cutoff, which leads to current jumps when the photon energy becomes too small to excite an electron to the lowest or from the highest available charge state in the dot.

To search for the effects presented above, we have used standard split-gate quantum dots⁸ defined in the two-dimensional electron gas (2DEG) of a GaAs/Al_xGa_{1-x}As heterostructure (see inset of Fig. 4). The mobility is 2.3×10^6 cm²/Vs and the electron density is 2×10^{15} m⁻² at 4 K. Besides applying dc voltages to all the gates, we

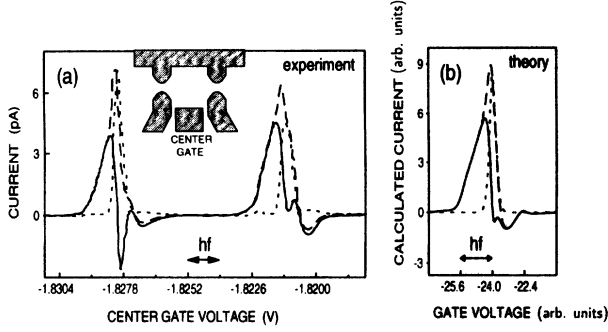


FIG. 4. (a) Measured $I-V_g$ with 19-GHz microwaves for $V_{sd} \sim 10 \mu\text{V}$. The inset schematically shows the gate structure. The dot diameter is about $0.5 \mu\text{m}$. (b) Calculated $I-V_g$ for $\alpha_s = 0.55$ and $\alpha_d = 0.4$, $k_B T/hf = 0.1$, $eV_{sd}/hf = 0.1$.

capacitively couple a microwave signal to the center gate. We use a tunable microwave source with a maximum frequency of 20 GHz. The microwaves are chopped with a frequency of 27 Hz, which allows a simultaneous measurement of the total current and the photocurrent. All measurements are done at a magnetic field of 2 T corresponding to a filling factor of 4 in the bulk 2DEG regions. Although the base temperature of the dilution refrigerator is 10 mK, the electron temperature is estimated to be about 100–150 mK. In this paper we only present data taken at 19.1 GHz, which corresponds to $hf = 80 \mu\text{eV}$. At this frequency the photon energy exceeds the thermal energy $k_B T$ by a factor of ~ 10 . Similar results were obtained at other frequencies.

For all the measurements that we present here, fixed voltages are applied to the barrier gates to make the tunnel conductances much smaller than e^2/h [of order $(M\Omega)^{-1}$]. In the absence of microwaves, we find a Coulomb staircase in current versus source-drain voltage characteristics from which we obtain a charging energy $e^2/C_{\text{tot}} \sim 0.45 \text{ meV}$. Keeping V_{sd} fixed and sweeping the center gate voltage we observe Coulomb oscillations with a period e/C_g between 7 and 7.5 mV. From these values we obtain a factor $C_g/C_{\text{tot}} = 0.062$ which converts the photon energy $hf = 80 \mu\text{eV}$ to 1.3 mV (within $\sim 20\%$ error) on the center gate voltage scale.

Figure 4(a) displays the effect of 19.1-GHz microwaves on two Coulomb oscillations measured with $V_{sd} \sim 10 \mu\text{V}$. The unpumped current (dotted) is the measured photocurrent (solid) subtracted from the measured pumped current (dashed). Both peaks show the same qualitative behavior. The microwave radiation increases the current on the left side and induces a negative current on the right side. Also shown are the results of our model for the parameters $eV_{sd}/hf = 0.1$, $k_B T/hf = 0.1$, and slightly asymmetric ac amplitudes $\alpha_s = 0.55$ and $\alpha_d = 0.4$. The calculation shown in Fig. 4(b) contains all the features observed in the experimental curve. From the comparison between the simulation and the experimental data we estimate the ac voltage amplitudes to be $\bar{V}_s, \bar{V}_d \sim 40 \mu\text{V}$.

Figure 5 shows a second example of a Coulomb peak measurement and its corresponding simulation. In this case, the measured broadening is almost symmetric and therefore simulated in Fig. 5(b) by equal ac voltage amplitudes

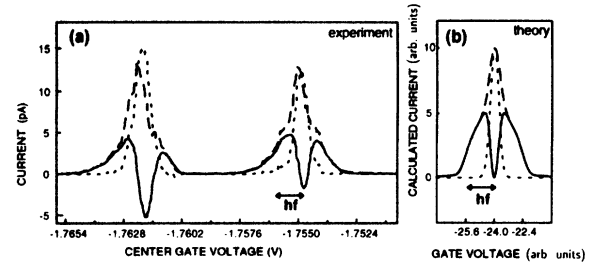


FIG. 5. (a) Measured $I-V_g$ with 19-GHz microwaves for $V_{sd} \sim 15 \mu\text{V}$. (b) Calculated $I-V_g$ for $\alpha_s = \alpha_d = 0.8$, $k_B T/hf = 0.1$, $eV_{sd}/hf = 0.4$.

$\alpha_s = \alpha_d = 0.4$. Again we find good agreement between measurement and our model.

As discussed earlier, it is possible to operate the quantum dot as an electron-photon pump. Figure 6 shows a measurement in which the pumped current (solid) at zero source-drain voltage is compared with a calculation (dashed). The calculation predicts a triangular shape for the small ac amplitude regime ($e\bar{V}/hf < 1$), which is also evident in the measurement. The photocurrent changes sign where the center of the normal peak is located (not shown), similar to the calculated curves in Fig. 2(b). We find that the photon energy size is somewhat larger in the calculation than expected from the experimental gate voltage scale. We would like to note, however, that it is not clear if it is justified to use a dc conversion factor for gate voltage to energy in a high-frequency measurement.

In summary, we have presented numerical simulations and measurements of photon-assisted tunneling in Coulomb blockade devices. The simulations provide a few clear predictions: (1) Multiphoton steps are predicted as additional structure in the differential Coulomb staircase and directly in Coulomb oscillations. (2) The double-junction system can operate as an electron-photon pump for unequal ac voltages. The measurements show clear microwave-induced features, and the observed photoresponse is in good agreement with our photon model. However, to conclusively demonstrate photonic excitation, it is necessary to increase the frequency relative to the temperature so that multiphoton current jumps can be identified and frequency scaling can be investigated.

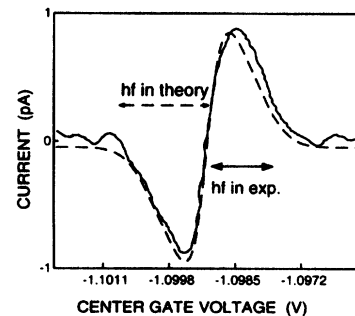


FIG. 6. Measured and calculated pumped current at $V_{sd} = 0$. Numerical parameters are $k_B T/hf = 0.2$, $\alpha_s = 0$, and $\alpha_d = 0.2$.

We would like to thank Bram van der Enden, Charlie Johnson, Chandu Karadi, Joe Orenstein, and Keith Wald for discussions and experimental help. This work was supported

by ONR, the Packard Foundation, NSF (K.M. and D.D.), the Sloan Foundation (P.L.M.), and the Royal Netherlands Academy of Arts and Sciences (L.P.K.).

*Present address: Department of Physics, University of Nottingham, Nottingham NG7 2RD, United Kingdom.

¹P. K. Tien and J. R. Gordon, *Phys. Rev.* **129**, 647 (1963).

²M. Buttiker and R. Landauer, *Phys. Rev. Lett.* **49**, 1739 (1982).

³P. Johansson, *Phys. Rev. B* **41**, 9892 (1990), and references therein.

⁴K. Flensberg, S. M. Girvin, M. Jonson, D. R. Penn, and M. D. Stiles, *Phys. Scr.* **T42**, 189 (1992).

⁵K. K. Likharev and I. A. Devyatov, *Physica B* **194-196**, 1341 (1994).

⁶A. Hadicke and W. Krech, *Physica B* **193**, 256 (1994).

⁷C. Bruder and H. Schoeller, *Phys. Rev. Lett.* **72**, 1076 (1994).

⁸See, for a recent collection of quantum dot papers, *The Physics of*

Few-Electron Nanostructures, edited by L. J. Geerligs, C. J. P. M. Harmans, and L. P. Kouwenhoven [*Physica B* **189** (1993)].

⁹L. P. Kouwenhoven, A. T. Johnson, N. C. van der Vaart, C. J. P. M. Harmans, and C. T. Foxon, *Phys. Rev. Lett.* **67**, 1626 (1991). In this turnstile experiment RF frequencies were used in the MHz regime for which $hf \ll k_B T$.

¹⁰D. V. Averin and K. K. Likharev, in *Mesoscopic Phenomena in Solids*, edited by B. L. Altshuler *et al.* (Elsevier, Amsterdam, 1991); G.-L. Ingold and Yu. V. Nazarov, in *Single Charge Tunneling*, edited by H. Grabert and M. H. Devoret (Plenum, New York, 1992).

¹¹F. Hekking and Yu. V. Nazarov, *Phys. Rev. B* **44**, 9110 (1991).

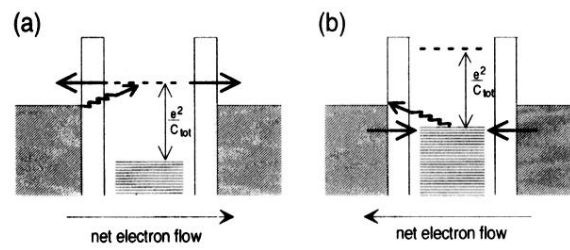


FIG. 3. Energy diagram for $V_{sd}=0$ and photon-assisted tunneling through only the left barrier. In (a) the resulting electron flow is from left to right, while in (b) it is from right to left.

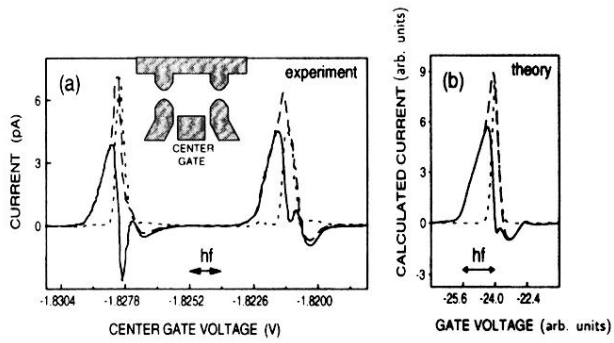


FIG. 4. (a) Measured $I-V_g$ with 19-GHz microwaves for $V_{sd} \sim 10 \mu\text{V}$. The inset schematically shows the gate structure. The dot diameter is about $0.5 \mu\text{m}$. (b) Calculated $I-V_g$ for $\alpha_s = 0.55$ and $\alpha_d = 0.4$, $k_B T/hf = 0.1$, $eV_{sd}/hf = 0.1$.